## Supporting Information

# Observability of paramagnetic NMR signals at over 10 000 ppm chemical shifts

*Jonas C. Ott, Elizaveta A. Suturina,\* Ilya Kuprov, Joscha Nehrkorn, Alexander Schnegg, Markus Enders,\* and Lutz H. Gade\**

anie_202107944_sm_miscellaneous_information.pdf

**Supporting Information**

## S1 General Procedures

*General Remarks*

All experiments were carried out in oven-dried glassware and under argon atmosphere by using standard Schlenk or glovebox techniques. Argon 5.0 from Messer Group GmbH was used as inert gas and dried over Granusic phosphorous pentoxide before usage. All solvents were purchased anhydrous from Honeywell and either collected from a solvent purification system (M. Braun SPS 800) after being dried over activated alumina columns or dried and degassed by using standard methods and stored in glass ampules with Teflon plugs under an atmosphere of argon. Deuterated solvents were purchased from Sigma-Aldrich, dried and vacuum distilled accordingly and degassed by at least three successive freeze-pump-thaw cycles. Samples for NMR spectroscopy were prepared under argon in a glovebox, transferred to 5mm Wilmad precision NMR tubes attached to a Schlenk-system and sealed with a butane lighter torch under slightly reduced pressure. NMR spectra were recorded on Bruker spectrometers (vide infra). $^1$H and $^{13}$C NMR spectra were referenced to residual solvent resonances and are given in parts per million (ppm) relative to external tetramethylsilane. Complex [$^{tBu}$(PNP)FeH] (**1**) was synthesized according to literature.[1]

*SQUID Magnetometry*

Magnetic susceptibility of **1** was measured from powder samples of solid material immobilized in eicosane (powder) or in toluene solution (solution) in the temperature range 2 – 290 K by using a Superconducting Quantum Interference Device (SQUID) with a field of 1 T (MPMS-7, Quantum Design, calibrated with standard palladium reference sample, error < 2%). To correct for the diamagnetic contribution of the solvent and sample holders, reference measurements were carried with empty samples holders and samples holders filled with solvent. Multiple-field variable-temperature magnetization measurements were done at 1, 4, and 7 T in the temperature range 2 – 260 K with the magnetization equidistantly sampled on a 1/T temperature scale.

*Computational Modelling*

Geometry optimization was performed with B3LYP/6-311G(d,p) + def2-TZVP (Fe only) methods and the hyperfine coupling tensors was calculated with range of DFT methods and basis sets indicated in the text for $C_s$ symmetrised geometry using Gaussian.[2] The diamagnetic shielding tensor was calculated with M06-L/6-31G(d)[3] for a structure where Fe was replaced with Zn and the diamagnetic shift was defined with respect to TMS reference. The magnetic susceptibility tensor was calculated with CASSCF(6,5)/NEVPT2 methods and def2-TZVP basis set with RI approximation where all 5 quintet, 45 triplet and 50 singlet states were included. These calculations and ab initio ligand field analysis were done with ORCA4.1.[4] Estimations of the spin-orbit effects on hyperfine were done with mean-field approximation and B3LYP/def2-TZVP basis set.

## S2 NMR Spectroscopy

*General Acquisition Procedure*

Unless stated otherwise, the spectra were recorded at a temperature of 295 K. Bruker and Magritec spectrometers (Magritek Spinsolve 60, Bruker DRX200, Bruker AVII 400, Bruker AVIII 600, Bruker AVIII 800) were used for the data collection. All temperature dependent $^1$H and $^{13}$C NMR spectra were recorded on a Bruker AVIII 600 MHz spectrometer equipped with a BBO probe (room temperature probe). The temperature of the measurements was calibrated using methanol and glycol (80% in DMSO) as standard substances.[5] Relaxation times were determined by the inverse-recovery method. Due to a non-uniform excitation profile of the 180° pulse within the inversion recovery pulse sequence, the measurements had to be performed with excitation frequencies near the resonance of the individual signals. For the detection of the $^{31}$P NMR signal the excitation frequency was set "on resonance". Moving the excitation frequency away from the resonance signal lead to disappearance of the signal. The identity of a real $^{31}$P NMR signal was verified by following the NMR shift at different temperatures and by measuring NMR tubes containing the solvent only. The data acquisition parameters used for the paramagnetic $^1$H, $^{13}$C and $^{31}$P NMR experiments are displayed in Tables S1-S3.

**Table S1.** Acquisition parameters for inverse-recovery $^1$H and $^{13}$C NMR experiments with different spectrometers.

| Spectrometer | DRX 200 | | AVII 400 | | AVIII 600 | | AVIII 800 | |
|---|---|---|---|---|---|---|---|---|
| Probe type | TBO | | BBFO | | BBO | | CP-TCI | |
| Nucleus | $^1$H | $^{13}$C | $^1$H | $^{13}$C | $^1$H | $^{13}$C | $^1$H | $^{13}$C |
| Pulse program (Bruker) | t1ir | t1irig | t1ir | t1irig | t1ir | t1irig | t1ir | t1irig |
| 90° pulse width $p1$ ($\mu$s) | 13.3 | 11.0 | 14.0 | 10.0 | 11.5 | 12.5 | 10.0 | 15.0 |
| acquisition time $aq$ (s) | 0.27 | 0.50 | 0.10 | 0.40 | 0.30 | 0.10 | 0.2 | 0.1 |
| Preacquisition delay $de$ ($\mu$s) | 4.5 | 15.5 | 4.5 | 18.0 | 6.5 | 18.0 | 10.0 | 18.0 |
| Number of scans $ns$ | 16 | 3k–30k | 16 | 256 – 2k | 16 | 1k – 2k | 8 | 64 – 128 |

**Table S2.** Acquisition parameters for $^1$H and $^{13}$C and $^{31}$P NMR experiments at room temperature (1.4 – 9.4 T).

| Spectrometer | Spinsolve 60 | DRX 200 | | | AVII 400 | | |
|---|---|---|---|---|---|---|---|
| Probe type | | TBO | | | BBFO | | |
| Nucleus | $^1$H | $^1$H | $^{13}$C | $^{31}$P | $^1$H | $^{13}$C | $^{31}$P |
| 90° pulse width $p1$ ($\mu$s) | 10.6 | 13.3 | 11.0 | 7.8 | 14.0 | 10.0 | 12.0 |
| Used pulse width | 10.6 | 4.4 | 7.3 | 7.8 | 1.4 | 6.7 | 12.0 |
| acquisition time $aq$ (s) | 0.65 | 0.44 | 0.43 | 0.03 | 0.50 | 0.16 | 0.02 |
| Relaxation delay $d1$ (s) | 1.0 | 0.05 | 0.2 | 0 | 0.05 | 0.20 | 0.02 |
| Preacq. delay $de$ ($\mu$s) | 20 | 6.0 | 20.0 | 6.0 | 6.5 | 6.5 | 4.5 |
| Number of scans $ns$ | 16 | 1k | 65k | 8k | 512 | 46k | 4k |

**Table S3.** Acquisition parameters for $^1H$ and $^{13}C$ and $^{31}P$ NMR experiments at room temperature (14.1 – 18.8 T).

| Spectrometer | AVIII 600 | | | | | AVIII 800 | |
|---|---|---|---|---|---|---|---|
| Probe type | BBO | | | CP-QNP | | CP-TCI | |
| Nucleus | $^1H$ | $^{13}C$ | $^{31}P$ | $^1H$ | $^{13}C$ | $^1H$ | $^{13}C$ |
| 90° pulse width $p1$ ($\mu$s) | 11.5 | 8.1 | 12.0 | 13.5 | 12.0 | 10.0 | 15.0 |
| Used pulse width | 1.2 | 5.4 | 12.0 | 1.4 | 8.0 | 1.0 | 5.0 |
| acquisition time $aq$ (s) | 0.40 | 0.20 | 0.03 | 0.1 | 0.16 | 0.2 | 0.16 |
| Relaxation delay $d1$ (s) | 1.0 | 0.05 | 0.0 | 1.0 | 0.05 | 1.0 | 0.5 |
| Preacq. delay $de$ ($\mu$s) | 6.5 | 6.5 | 6.0 | 10.0 | 18.0 | 10.0 | 18.0 |
| Number of scans $ns$ | 128 | 20k | 16k | 128 | 4k | 8 | 1k |

**Table S4.** $R_1$ relaxation rates of selected nuclei of complex **1** at various external fields in Hz.

| B (T) | 18.8 | 14.1 | 9.4 | 4.7 | 1.4 |
|---|---|---|---|---|---|
| $C^6$ | 88.5 | 62.1 | 34.1 | 10.9 | |
| $C^1$ | 52.9 | 33.9 | 17.8 | 5.2 | |
| $H^2$ | 48.5 | 34.2 | 18.8 | 6.2 | 1.6 |
| $C^{11}$ | 43.7 | 26.3 | 13.4 | 6.1 | |
| $H^4$ | 28.6 | 19.6 | 10.8 | 3.5 | 1.2 |
| $C^5$ | 21.2 | 13.7 | 6.3 | 2.6 | |
| $C^2$ | 9.5 | 7.2 | 5.2 | 2.3 | |
| $C^4$ | 8.5 | 5.8 | 3.8 | 2.3 | |
| $C^3$ | 8.3 | 5.2 | 3.1 | 2.8 | |
| $C^8$ | 3.0 | 1.9 | 1.3 | 1.2 | |
| $C^7$ | 1.7 | 0.6 | 0.3 | 0.2 | |

**Table S5.** Chemical shifts (600.1 MHz, Tol-$d^8$) of the $^1$H NMR resonances of complex **1** at various temperatures.

| T (K) | H$^4$ | H$^2$ | H$^8$ | H$^{11}$ | H$^9$ | H$^{12}$ |
|---|---|---|---|---|---|---|
| 217.93 | 25.41 | 7.36 | 4.81 | -9.61 | -95.4 | -4783 |
| 223.13 | 25.01 | 7.41 | 4.73 | -9.35 | -93.3 | -4676 |
| 228.35 | 24.63 | 7.45 | 4.66 | -9.13 | -91.0 | -4572 |
| 233.13 | 24.27 | 7.49 | 4.59 | -8.92 | -89.0 | -4474 |
| 238.91 | 23.92 | 7.52 | 4.53 | -8.70 | -86.3 | -4385 |
| 244.09 | 23.60 | 7.56 | 4.47 | -8.51 | -84.2 | -4289 |
| 249.34 | 23.29 | 7.59 | 4.41 | -8.33 | -82.1 | -4199 |
| 254.59 | 22.99 | 7.62 | 4.35 | -8.15 | -80.4 | -4114 |
| 259.89 | 22.71 | 7.64 | 4.30 | -7.99 | -78.7 | -4032 |
| 265.16 | 22.44 | 7.67 | 4.24 | -7.83 | -76.9 | -3952 |
| 270.48 | 22.19 | 7.69 | 4.19 | -7.68 | -75.3 | -3877 |
| 275.78 | 21.94 | 7.71 | 4.14 | -7.54 | -73.7 | -3803 |
| 281.05 | 21.71 | 7.73 | 4.10 | -7.40 | -72.2 | -3733 |
| 286.38 | 21.49 | 7.74 | 4.05 | -7.27 | -70.8 | -3667 |
| 291.75 | 21.28 | 7.76 | 4.01 | -7.14 | -69.4 | -3598 |
| 297.17 | 21.05 | 7.78 | 3.97 | -7.00 | -67.9 | -3529 |
| 302.77 | 20.88 | 7.79 | 3.93 | -6.89 | -66.8 | -3475 |
| 307.90 | 20.69 | 7.80 | 3.89 | -6.78 | -65.5 | -3415 |
| 313.07 | 20.51 | 7.81 | 3.86 | -6.67 | -64.4 | -3356 |
| 318.30 | 20.34 | 7.82 | 3.82 | -6.57 | -63.2 | -3301 |
| 323.51 | 20.17 | 7.83 | 3.79 | -6.47 | -62.1 | -3247 |
| 328.68 | 20.01 | 7.84 | 3.76 | -6.37 | -61.1 | -3195 |
| 333.84 | 19.86 | 7.85 | 3.73 | -6.28 | -60.0 | -3144 |
| 338.97 | 19.71 | 7.86 | 3.69 | -6.19 | -59.0 | -3088 |
| 344.22 | 19.57 | 7.87 | 3.67 | -6.10 | -58.1 | -3048 |

**Table S6.** Chemical shifts (150.9 MHz, Tol-$d^8$) of the $^{13}$C NMR resonances of complex **1** at various temperatures.

| T (K) | C$^3$ | C$^1$ | C$^5$ | C$^{11}$ | C$^8$ | C$^2$ | C$^4$ | C$^7$ | C$^6$ | C$^{10}$ | C$^9$ |
|---|---|---|---|---|---|---|---|---|---|---|---|
| 217.93 | 270.3 | 208.9 | 203.6 | n.o. | 74.0 | 32.4 | 8.4 | -2.8 | -226.7 | -570.2 | -1312.7 |
| 223.13 | 267.4 | 207.1 | 202.1 | n.o. | 73.1 | 34.4 | 10.8 | -2.0 | -217.7 | -556.6 | -1280.7 |
| 228.35 | 264.6 | 205.4 | 200.7 | n.o. | 72.3 | 36.2 | 13.2 | -1.2 | -209.3 | -543.2 | -1251.2 |
| 233.13 | 261.9 | 203.8 | 199.3 | n.o. | 71.5 | 38.1 | 15.5 | -0.4 | -201.1 | -530.3 | -1222.6 |
| 238.91 | 259.3 | 202.2 | 198.0 | n.o. | 70.7 | 39.8 | 17.7 | 0.4 | -193.2 | -517.7 | -1194.7 |
| 244.09 | 256.8 | 200.7 | 196.8 | n.o. | 69.9 | 41.5 | 19.9 | 1.1 | -185.3 | -505.4 | -1167.5 |
| 249.34 | 254.5 | 199.3 | 195.7 | n.o. | 69.2 | 43.1 | 21.9 | 1.8 | -177.9 | -494.0 | -1141.3 |
| 254.59 | 252.2 | 197.9 | 194.6 | 118.1 | 68.5 | 44.7 | 23.9 | 2.5 | -170.7 | -483.0 | -1117.1 |
| 259.89 | 250.0 | 196.6 | 193.6 | 117.4 | 67.8 | 46.2 | 25.8 | 3.1 | -163.8 | -472.3 | -1093.7 |
| 265.16 | 247.9 | 195.3 | 192.6 | 115.8 | 67.2 | 47.7 | 27.7 | 3.8 | -157.2 | -462.1 | -1071.0 |
| 270.48 | 245.9 | 194.1 | 191.7 | 114.3 | 66.5 | 49.1 | 29.4 | 4.4 | -150.7 | -452.4 | -1049.2 |
| 275.78 | 243.9 | 193.0 | 190.8 | 112.2 | 65.9 | 50.4 | 31.1 | 4.9 | -144.5 | -443.0 | -1028.0 |
| 281.05 | 242.1 | 191.8 | 190.0 | 111.0 | 65.4 | 51.7 | 32.8 | 5.5 | -138.6 | -434.1 | -1008.2 |
| 286.38 | 240.3 | 190.8 | 189.2 | 109.2 | 64.8 | 52.9 | 34.4 | 6.0 | -132.8 | -425.3 | -988.2 |
| 291.75 | 238.6 | 189.7 | 188.5 | 108.1 | 64.3 | 54.2 | 35.9 | 6.6 | -127.2 | -417.0 | -969.7 |
| 297.17 | 236.8 | 188.7 | 187.7 | 107.0 | 63.7 | 55.4 | 37.5 | 7.1 | -121.5 | -408.6 | -951.0 |
| 302.77 | 235.3 | 187.7 | 187.1 | 105.3 | 63.3 | 56.5 | 38.9 | 7.6 | -116.5 | -401.1 | -934.4 |
| 307.90 | 233.8 | 186.8 | 186.5 | 104.2 | 62.8 | 57.6 | 40.3 | 8.0 | -111.4 | -393.6 | -916.8 |
| 313.07 | 232.3 | 185.9 | 185.9 | 102.9 | 62.3 | 58.6 | 41.6 | 8.5 | -106.5 | -386.3 | -900.7 |
| 318.30 | 230.8 | 185.0 | 185.3 | 101.8 | 61.9 | 59.7 | 42.9 | 9.0 | -101.8 | -379.2 | -885.0 |
| 323.51 | 229.5 | 184.2 | 184.7 | 100.6 | 61.4 | 60.7 | 44.2 | 9.4 | -97.2 | -372.5 | -870.6 |
| 328.68 | 228.1 | 183.4 | 184.2 | 99.4 | 61.0 | 61.7 | 45.5 | 9.8 | -92.7 | -365.9 | -856.3 |
| 333.84 | 226.8 | 182.6 | 183.7 | 98.5 | 60.6 | 62.6 | 46.7 | 10.2 | -88.3 | -359.4 | -841.3 |
| 338.97 | 225.5 | 181.8 | 183.2 | 97.4 | 60.2 | 63.5 | 47.8 | 10.6 | -84.0 | -353.3 | -827.8 |
| 344.22 | 224.3 | 181.1 | 182.7 | 96.4 | 59.8 | 64.4 | 49.0 | 11.0 | -79.8 | -347.3 | -814.0 |
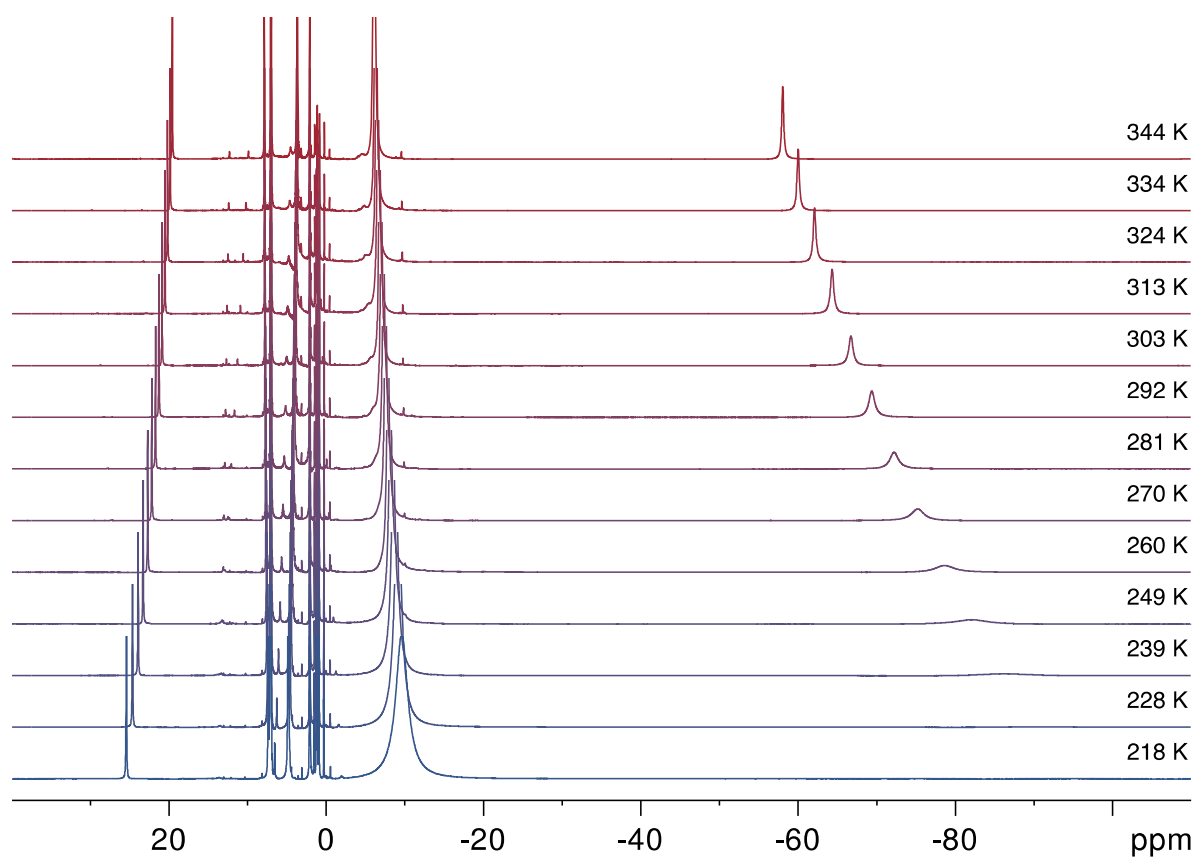
**Figure S1.** $^1$H NMR spectra (600.1 MHz, Tol-$d^8$) of complex **1** at various temperatures.
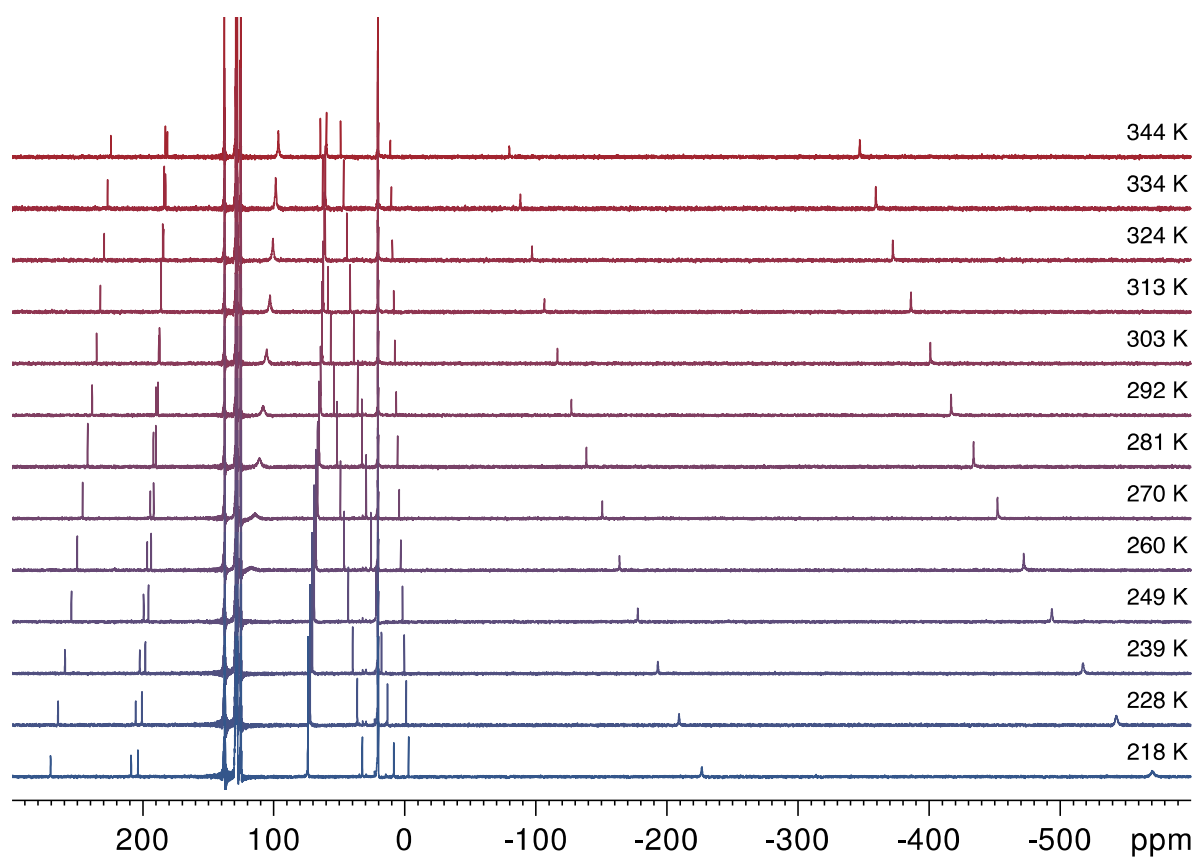
**Figure S2.** $^{13}C$ NMR spectra (150.9 MHz, Tol-$d^8$) of complex **1** at various temperatures.
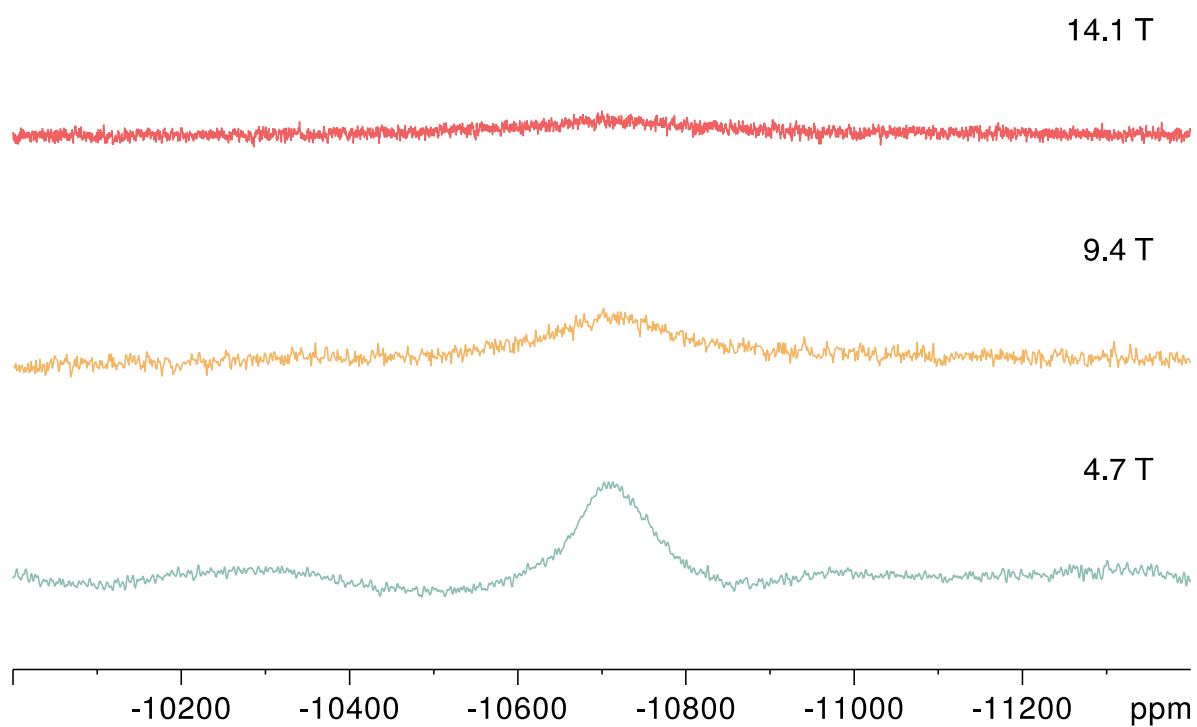
**Figure S3.** $^{31}$P NMR spectra (295 K, Tol-$d^8$) of complex **1** at various external fields.

## S3 FD-FT THz-EPR Spectroscopy

FD-FT THz-EPR was performed at the THz beamline of the synchrotron BESSY II, Helmholtz-Zentrum Berlin, Germany.[6] This spectrometer allows for THz-EPR measurements from ~ 0.1 to 11 THz (~ 3 – 370 cm$^{-1}$) employing a fully evacuated quasi-optical beam path, a high-resolution FTIR spectrometer (IFS 125, Bruker), a superconducting high field magnet (Oxford Spectromag 4000, $B_0$ = +11 T - 11T) with variable temperature insert ($T$ = 1.5 K – 300 K) and liquid He cooled bolometer detectors. Herein, the internal source of the FTIR spectrometer (Hg arc lamp) was used as THz source in combination with a pumped liquid He cooled (1.5 K) bolometer. This set-up is most sensitive in the frequency range between 17 and 45 cm$^{-1}$. A larger spectral window, yet significantly lower detection sensitivity, is achieved between ~ 20 and 370 cm$^{-1}$ employing a bolometer operated at 4.2 K. A detailed description of the spectrometer can be found elsewhere.[7,8] Samples were measured as pellets (15.9 mg powder sample of **1** and 117.8 mg Polyethylene), pressed inside a glove box, vacuum-sealed and immediately frozen in liquid nitrogen. SH simulations were performed with EasySpin[9] and its extension for frequency-domain EPR.[10]
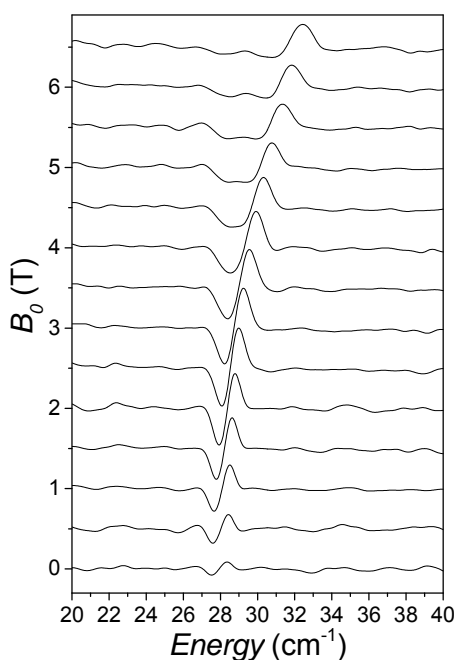


**Figure S4.** Magnetic Division Spectra (MDS) FD-FT THz-EPR spectra of pressed powder pellets of **1** measured at a temperature of 5 K. The MDS for the magnetic field $B_0$ is obtained by dividing the raw spectrum measured at $B_0$ by the spectrum measured at $B_0$ + 1 T. Data is shown offset for $B_0$ and rescaled with a global normalization factor. In MDS, EPR resonances appear as negative (EPR resonance at $B_0$) and positive (EPR resonance at $B_0$ + 1 T) deviations from **1**.
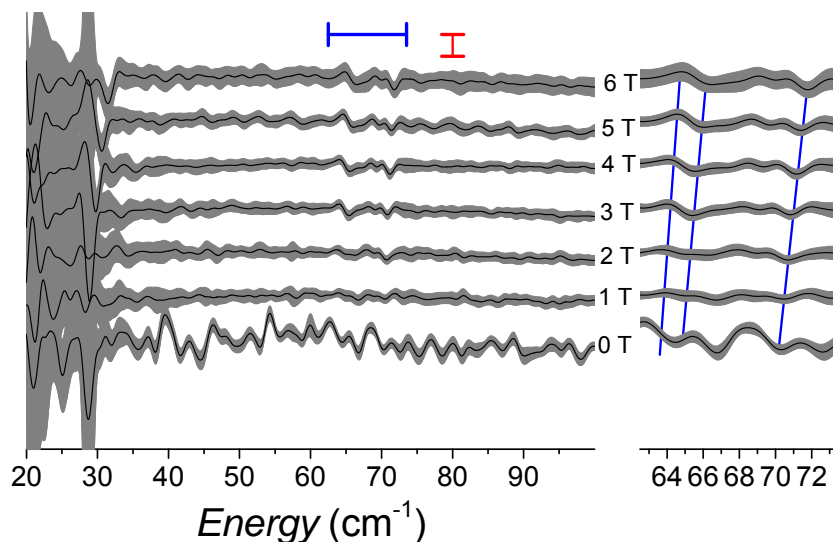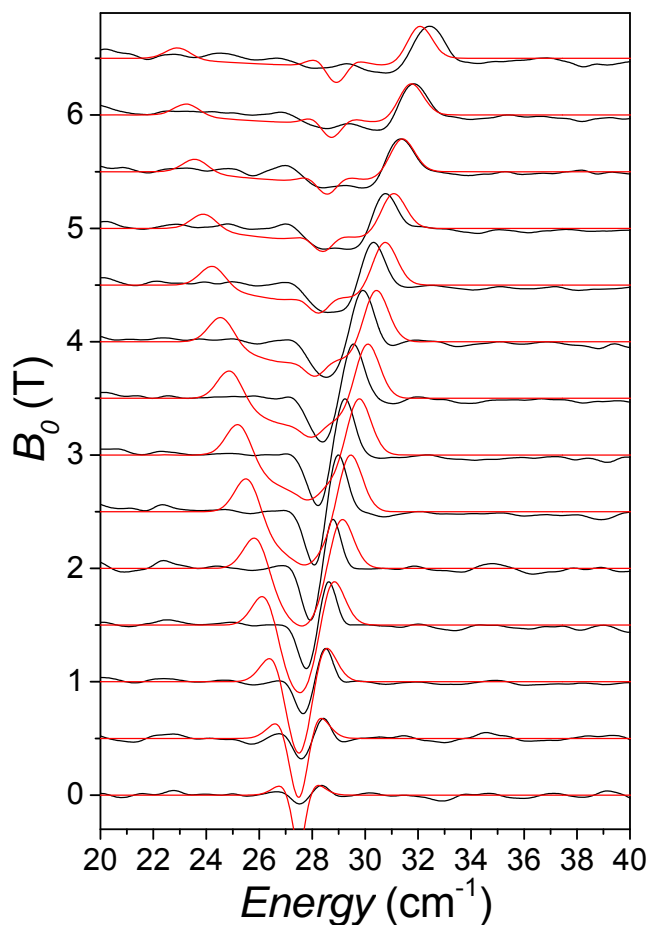
**Figure S5.** Magnetic Division Spectra (MDS) FD-FT THz-EPR spectra of pressed powder pellets of **1** measured at a temperature of 5 K. The gray shaded area marks the uncertainty obtained from the standard deviation of the recorded spectra. The red bar denotes 1%. The blue bar in the second plot marks the region that is shown magnified on the right side. Blue lines are guide to the eye to follow the magnetic field dependent spectral features.

Figure S4 depicts field dependent FD-FT THz-EPR spectra measured with a 1.5 K Si bolometer. At zero magnetic field a single EPR resonance at 27.5 cm$^{-1}$ is observed. Upon application of an external magnetic field, this resonance shifts to higher excitation energies. Notably, the field dependence is clearly nonlinear. In addition, FD-FT THz EPR spectra were recorded with the broadband spectrometer configuration employing a Hg arc lamp as THz source and a bolometer cooled to 4.2 K. In the spectra depicted in Figure S5 three field-dependent features have been observed between 64 and 70 cm$^{-1}$. However, due to the much lower detection sensitivity in this frequency range, these features are much less pronounced. A direct comparison of the transitions depicted in Figure S4 and Figure S5 is difficult due to the differences in the detection sensitivity of the two detection modes.

**Figure S6.** Experimental (black, same data as in Figure S1) and simulated (red ) FD-FT THz-EPR magnetic division spectra (MDS) of pressed powder samples of **1** measured at T = 5 K. Simulations with Eq 8[4] were obtained with SH parameters: $D = 27.5$ cm$^{-1}$, $E = 0$, and an isotropic g = 1.4. The field dependence of the high-energy line remain linear even for anisotropic g values (simulations not shown).

The simplest interpretation for the resonance at 27.5 cm$^{-1}$ for $S = 1$ is an axial ZFS with $D = 27.5$ cm$^{-1}$ and vanishing $E$. However, simulations of the field dependent spectra with this parameter set deviate significantly from the experimental spectra (see Figure S6). First, the simulations do not reproduce the relative intensities observed with and without field, Furthermore, the position of the high-energy maximum increases linearly with increasing magnetic field in the simulation, which was not observed experimentally. Therefore, we discarded axial ZFS from the further considerations.

# S4 SQUID MAGNETOMETRY
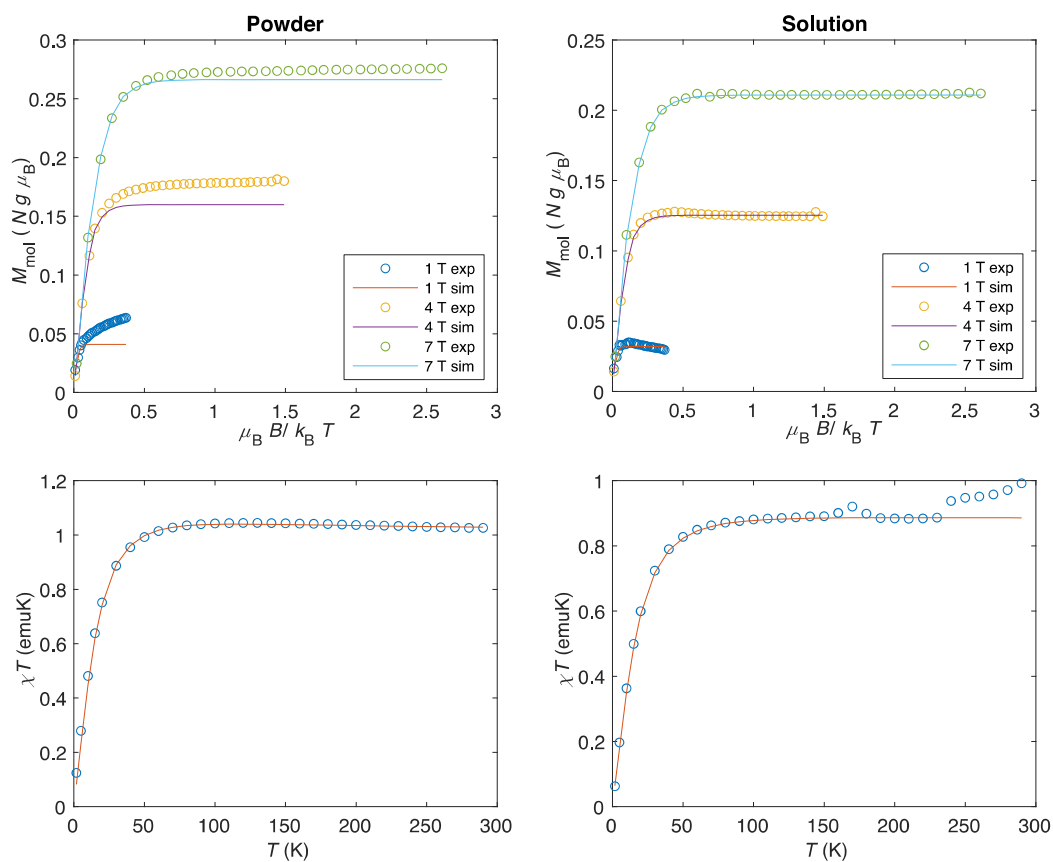


**Figure S7.** Experimental (circles) and simulated (solid lines) reduced magnetisation at 1 T, 4 T and 7 T of complex **1** as powder (top left) and in toluene solution (top right) with a concentration of $9.67 \times 10^{-2}$ mol/l. Magnetic susceptibility is shown as $\chi T$ product vs. temperature for powder (bottom left) and solution (bottom right). Simulations were obtained with $D = -54$ cm$^{-1}$, $|E| = 14$ cm$^{-1}$, ($|E/D| = 0.26$), $g_\perp = 1.72$, $g_\parallel = 2.49$ and a TIP of 0.0015 emu, for the powder samples and $D = -54$ cm$^{-1}$, $|E| = 14$ cm$^{-1}$, ($|E/D| = 0.26$), $g_x = 1.40$, $g_y = 1.90$, $g_z = 2.23$ and a TIP of 0.00059 emu for the solution samples.

# S5 NMR SHIFT ANALYSIS

**Table S7.** Atomic coordinates (in Å) of DFT (B3LYP/6-311G(d,p) + def2-TZVP(Fe only)) S = 1 optimized symmetrized molecular structure, components of hyperfine tensor computed with TPSSH/def2-TZVP with dipolar part normalized per electron (ppm/Å$^3$) and diamagnetic shielding calculated for S = 0 with M06-L/6-31G(d) in ppm not adjusted for reference (189.6621 ppm for carbon and 32.1833 ppm for hydrogen). Both hyperfine and shielding tensors are symmetric and only unique components are shown.

| Atom | X | Y | Z | $A_{xx}$ | $A_{xy}$ | $A_{xz}$ | $A_{yy}$ | $A_{yz}$ | $A_{zz}$ | $\sigma_{xx}$ | $\sigma_{xy}$ | $\sigma_{xz}$ | $\sigma_{yy}$ | $\sigma_{yz}$ | $\sigma_{zz}$ |
|---|---|---|---|---|---|---|---|---|---|---|---|---|---|---|---|
| Fe | 0 | 0 | 0 | 1521048 | 0 | −14934 | 615903 | 0 | 2286466 | −14126 | 0 | 5379 | −48808 | 0 | −14000 |
| P | 0.21545 | 2.27554 | 0.08741 | −123751 | −5276 | −918 | −155188 | −2238 | −124037 | 182 | −12 | 29 | 211 | 25 | 165 |
| P | 0.21545 | −2.27554 | 0.08741 | −123751 | 5276 | −918 | −155188 | 2238 | −124037 | 182 | 12 | 29 | 211 | −25 | 165 |
| N | −2.01928 | 0 | −0.23098 | −40185 | 0 | −4534 | −55238 | 0 | −34669 | −72 | 0 | −97 | 186 | 0 | 208 |
| C | −2.77544 | −1.10878 | −0.63527 | −1638 | 2729 | 837 | −7628 | 88 | −8690 | 30 | −28 | −60 | 7 | −3 | 97 |
| C | −2.56495 | −2.48524 | −0.41042 | 1443 | 2366 | −994 | 760 | 619 | 349 | 56 | −7 | −75 | 18 | 9 | 111 |
| C | −3.4809 | −3.38823 | −0.95139 | −977 | 962 | 615 | −760 | 310 | −2141 | 90 | 10 | −39 | −14 | 17 | 120 |
| C | −4.61526 | −3.01363 | −1.6984 | 1465 | 526 | −1360 | −20 | 259 | 2304 | 37 | −20 | −79 | 1 | −1 | 111 |
| C | −4.83392 | −1.65101 | −1.8799 | −699 | 455 | 993 | −1273 | 107 | −2250 | 42 | 6 | −82 | 57 | 11 | 122 |
| C | −3.93864 | −0.7186 | −1.35237 | 1707 | 522 | −948 | −2160 | 350 | −14 | 53 | −1 | −61 | −8 | 3 | 122 |
| C | −3.93864 | 0.7186 | −1.35237 | 1707 | −522 | −948 | −2160 | −350 | −14 | 53 | 1 | −61 | −8 | −3 | 122 |
| C | −4.83392 | 1.65101 | −1.8799 | −699 | −455 | 993 | −1273 | −107 | −2250 | 42 | −6 | −82 | 57 | −11 | 122 |
| C | −4.61526 | 3.01363 | −1.6984 | 1465 | −526 | −1360 | −20 | −259 | 2304 | 37 | 20 | −79 | 1 | 1 | 111 |
| C | −3.4809 | 3.38823 | −0.95139 | −977 | −962 | 615 | −760 | −310 | −2141 | 90 | −10 | −39 | −14 | −17 | 120 |
| C | −2.56495 | 2.48524 | −0.41042 | 1443 | −2366 | −994 | 760 | −619 | 349 | 56 | 7 | −75 | 18 | −9 | 111 |
| C | −2.77544 | 1.10878 | −0.63527 | −1638 | −2729 | 837 | −7628 | −88 | −8690 | 30 | 28 | −60 | 7 | 3 | 97 |
| C | −1.45033 | 3.01426 | 0.45334 | −16935 | −710 | 369 | −11076 | 161 | −15267 | 162 | 15 | 13 | 124 | −2 | 168 |
| C | −1.45033 | −3.01426 | 0.45334 | −16935 | 710 | 369 | −11076 | −161 | −15267 | 162 | −15 | 13 | 124 | 2 | 168 |
| C | −5.5765 | −4.07112 | −2.27313 | −374 | 280 | 130 | −533 | 118 | −656 | 143 | 4 | −1 | 150 | 2 | 141 |
| C | −5.10992 | −5.4979 | −1.9203 | 35 | 245 | 79 | 123 | 92 | −145 | 146 | −11 | 5 | 167 | −8 | 142 |
| C | −6.99417 | −3.85935 | −1.69292 | 1136 | 199 | 56 | 774 | 40 | 695 | 172 | −4 | −14 | 141 | 4 | 140 |
| C | −5.6531 | −3.96469 | −3.80983 | 859 | 186 | 211 | 724 | 137 | 850 | 133 | 3 | 4 | 140 | −2 | 178 |
| C | −5.5765 | 4.07112 | −2.27313 | −374 | −280 | 130 | −533 | −118 | −656 | 143 | −4 | −1 | 150 | −2 | 141 |
| C | −5.6531 | 3.96469 | −3.80983 | 859 | −186 | 211 | 724 | −137 | 850 | 133 | −3 | 4 | 140 | 2 | 178 |
| C | −6.99417 | 3.85935 | −1.69292 | 1136 | −199 | 56 | 774 | −40 | 695 | 172 | 4 | −14 | 141 | −4 | 140 |
| C | −5.10992 | 5.4979 | −1.9203 | 35 | −245 | 79 | 123 | −92 | −145 | 146 | 11 | 5 | 167 | 8 | 142 |
| C | 1.25694 | 2.90266 | 1.5762 | −6895 | 1261 | 67 | −3569 | 1209 | −7282 | 144 | −2 | 4 | 120 | −6 | 150 |
| C | 0.51742 | 2.43218 | 2.84568 | 981 | 593 | 469 | 3864 | 2367 | 3197 | 148 | 9 | −15 | 138 | −21 | 164 |
| C | 2.65597 | 2.26203 | 1.58582 | 1505 | 1979 | 1115 | 632 | 778 | −45 | 168 | −23 | −1 | 146 | 0 | 144 |
| C | 1.39787 | 4.43437 | 1.63482 | −2986 | 412 | 164 | −2205 | 417 | −2929 | 142 | 0 | −1 | 164 | −6 | 148 |
| C | 0.79072 | 3.07297 | −1.55837 | −7843 | 772 | −1 | −4246 | −990 | −8398 | 142 | −3 | −5 | 112 | 3 | 148 |
| C | −0.28186 | 2.72238 | −2.60889 | −670 | −291 | 151 | 2314 | −2180 | 1116 | 163 | 12 | 17 | 134 | 20 | 161 |
| C | 2.1201 | 2.45246 | −2.02115 | 784 | 1757 | −1202 | 1608 | −1361 | 462 | 166 | −22 | −7 | 142 | 11 | 142 |
| C | 0.9293 | 4.60339 | −1.48825 | −3106 | 252 | −90 | −2230 | −401 | −2977 | 145 | 1 | 3 | 162 | 8 | 149 |
| C | 1.25694 | −2.90266 | 1.5762 | −6895 | −1261 | 67 | −3569 | −1209 | −7282 | 144 | 2 | 4 | 120 | 6 | 150 |
| C | 0.51742 | −2.43218 | 2.84568 | 981 | −593 | 469 | 3864 | −2367 | 3197 | 148 | −9 | −15 | 138 | 21 | 164 |
| C | 2.65597 | −2.26203 | 1.58582 | 1505 | −1979 | 1115 | 632 | −778 | −45 | 168 | 23 | −1 | 146 | 0 | 144 |
| C | 1.39787 | −4.43437 | 1.63482 | −2986 | −412 | 164 | −2205 | −417 | −2929 | 142 | 0 | −1 | 164 | 6 | 148 |
| C | 0.79072 | −3.07297 | −1.55837 | −7843 | −772 | −1 | −4246 | 990 | −8398 | 142 | 3 | −5 | 112 | −3 | 148 |
| C | −0.28186 | −2.72238 | −2.60889 | −670 | 291 | 151 | 2314 | 2180 | 1116 | 163 | −12 | 17 | 134 | −20 | 161 |
| C | 2.1201 | −2.45246 | −2.02115 | 784 | −1757 | −1202 | 1608 | 1361 | 462 | 166 | 22 | −7 | 142 | −11 | 142 |
| C | 0.9293 | −4.60339 | −1.48825 | −3106 | −252 | −90 | −2230 | 401 | −2977 | 145 | −1 | 3 | 162 | −8 | 149 |
| H | 1.57026 | 0 | 0 | −26015 | 0 | −97 | −91134 | 0 | −83045 | −111 | 0 | 9 | 245 | 0 | 86 |
| H | −3.30318 | −4.44077 | −0.7616 | 24 | 639 | 95 | 488 | 143 | −376 | 30 | 1 | 5 | 19 | 1 | 23 |
| H | −5.70112 | −1.29706 | −2.42497 | 453 | 214 | 335 | −209 | 91 | −191 | 22 | 1 | 2 | 34 | 1 | 19 |
| H | −5.70112 | 1.29706 | −2.42497 | 453 | −214 | 335 | −209 | −91 | −191 | 22 | −1 | 2 | 34 | −1 | 19 |
| H | −3.30318 | 4.44077 | −0.7616 | 24 | −639 | 95 | 488 | −143 | −376 | 30 | −1 | 5 | 19 | −1 | 23 |
| H | −1.64364 | 2.73015 | 1.49155 | 138 | −1985 | −731 | 2609 | 1767 | −190 | 29 | 13 | 4 | 11 | −11 | 34 |

| H | −1.43308 | 4.10448 | 0.4183 | −3318 | −800 | 6 | −1172 | 261 | −3339 | 32 | 3 | 2 | 17 | −1 | 27 |
|---|---|---|---|---|---|---|---|---|---|---|---|---|---|---|---|
| H | −1.43308 | −4.10448 | 0.4183 | −3318 | 800 | 6 | −1172 | −261 | −3339 | 32 | −3 | 2 | 17 | 1 | 27 |
| H | −1.64364 | −2.73015 | 1.49155 | 138 | 1985 | −731 | 2609 | −1767 | −190 | 29 | −13 | 4 | 11 | 11 | 34 |
| H | −5.80116 | −6.23359 | −2.33991 | 15 | 164 | 58 | 62 | 66 | −104 | 30 | 2 | 2 | 35 | 1 | 28 |
| H | −5.07334 | −5.65628 | −0.84 | 32 | 260 | 34 | 136 | 36 | −178 | 29 | 0 | 2 | 30 | −4 | 31 |
| H | −4.1164 | −5.70234 | −2.32727 | −37 | 241 | 93 | 175 | 141 | −151 | 33 | −4 | 1 | 30 | 1 | 27 |
| H | −7.68919 | −4.60272 | −2.09688 | 185 | 141 | 60 | 46 | 40 | −23 | 35 | 3 | 1 | 30 | 0 | 27 |
| H | −7.37887 | −2.86725 | −1.94132 | 227 | 138 | 101 | −105 | 39 | −143 | 33 | −3 | 0 | 34 | 0 | 25 |
| H | −6.99514 | −3.95327 | −0.60398 | 189 | 214 | 15 | −59 | 14 | −159 | 32 | 0 | −3 | 29 | −1 | 33 |
| H | −6.34002 | −4.71785 | −4.20533 | 114 | 136 | 116 | 46 | 91 | 25 | 29 | 2 | 4 | 30 | 2 | 33 |
| H | −4.67444 | −4.12973 | −4.26807 | 5 | 194 | 186 | −31 | 191 | −3 | 31 | −1 | −2 | 28 | 1 | 34 |
| H | −6.01423 | −2.98468 | −4.12849 | 108 | 145 | 211 | −108 | 96 | −29 | 27 | −2 | 3 | 33 | −3 | 32 |
| H | −6.34002 | 4.71785 | −4.20533 | 114 | −136 | 116 | 46 | −91 | 25 | 29 | −2 | 4 | 30 | −2 | 33 |
| H | −6.01423 | 2.98468 | −4.12849 | 108 | −145 | 211 | −108 | −96 | −29 | 27 | 2 | 3 | 33 | 3 | 32 |
| H | −4.67444 | 4.12973 | −4.26807 | 5 | −194 | 186 | −31 | −191 | −3 | 31 | 1 | −2 | 28 | −1 | 34 |
| H | −7.68919 | 4.60272 | −2.09688 | 185 | −141 | 60 | 46 | −40 | −23 | 35 | −3 | 1 | 30 | 0 | 27 |
| H | −6.99514 | 3.95327 | −0.60398 | 189 | −214 | 15 | −59 | −14 | −159 | 32 | 0 | −3 | 29 | 1 | 33 |
| H | −7.37887 | 2.86725 | −1.94132 | 227 | −138 | 101 | −105 | −39 | −143 | 33 | 3 | 0 | 34 | 0 | 25 |
| H | −5.80116 | 6.23359 | −2.33991 | 15 | −164 | 58 | 62 | −66 | −104 | 30 | −2 | 2 | 35 | −1 | 28 |
| H | −4.1164 | 5.70234 | −2.32727 | −37 | −241 | 93 | 175 | −141 | −151 | 33 | 4 | 1 | 30 | −1 | 27 |
| H | −5.07334 | 5.65628 | −0.84 | 32 | −260 | 34 | 136 | −36 | −178 | 29 | 0 | 2 | 30 | 4 | 31 |
| H | 0.38221 | 1.34891 | 2.85878 | −2658 | 530 | 918 | −732 | 3521 | 3574 | 33 | 1 | −1 | 46 | −20 | 23 |
| H | −0.4574 | 2.89943 | 2.95812 | −1103 | −292 | −215 | 632 | 1691 | 308 | 35 | 1 | 0 | 22 | −9 | 31 |
| H | 1.1086 | 2.69966 | 3.72165 | −561 | 352 | 469 | 131 | 1088 | 663 | 30 | −1 | 1 | 29 | −5 | 36 |
| H | 2.60366 | 1.17663 | 1.51112 | 2568 | 2265 | 2376 | −1607 | 905 | −1332 | 25 | −13 | −3 | 48 | −4 | 30 |
| H | 3.15175 | 2.51671 | 2.52481 | 91 | 838 | 726 | −270 | 601 | −346 | 34 | −4 | 3 | 30 | −2 | 33 |
| H | 3.28573 | 2.62549 | 0.77826 | 788 | 1399 | 358 | 127 | 283 | −787 | 33 | −8 | −3 | 26 | −2 | 33 |
| H | 1.96169 | 4.83461 | 0.79132 | −270 | 487 | 84 | 804 | 211 | −439 | 27 | 1 | 0 | 22 | −3 | 34 |
| H | 1.94005 | 4.70724 | 2.54617 | −577 | 363 | 156 | 147 | 436 | −514 | 30 | 1 | 2 | 28 | 1 | 32 |
| H | 0.43171 | 4.94021 | 1.67127 | −486 | 152 | 25 | 932 | 414 | −318 | 31 | −3 | 1 | 25 | −1 | 29 |
| H | −1.24576 | 3.16841 | −2.38185 | −758 | −764 | 444 | 958 | −1424 | −128 | 42 | 3 | −4 | 18 | 5 | 29 |
| H | −0.42162 | 1.64235 | −2.70311 | −2463 | −616 | 863 | −71 | −3665 | 2611 | 39 | 4 | −2 | 37 | 19 | 24 |
| H | 0.04322 | 3.09931 | −3.58082 | −683 | 21 | −54 | 370 | −1161 | 540 | 32 | 0 | 0 | 27 | 4 | 36 |
| H | 2.95864 | 2.742 | −1.39344 | 421 | 1370 | −592 | 207 | −565 | −691 | 34 | −8 | 2 | 25 | 4 | 31 |
| H | 2.33409 | 2.80235 | −3.0336 | −233 | 708 | −676 | 39 | −847 | 79 | 32 | −4 | −3 | 28 | 4 | 33 |
| H | 2.07293 | 1.36254 | −2.04384 | 836 | 2367 | −2999 | −1019 | −1918 | 2 | 23 | −15 | 5 | 45 | 12 | 23 |
| H | −0.00816 | 5.0863 | −1.20662 | −501 | 46 | 26 | 970 | −313 | −408 | 32 | −2 | −1 | 24 | 1 | 28 |
| H | 1.20475 | 4.98264 | −2.4785 | −880 | 235 | −92 | 6 | −449 | −781 | 29 | 0 | −2 | 28 | −1 | 32 |
| H | 1.70628 | 4.92303 | −0.79188 | −331 | 422 | −85 | 849 | −211 | −442 | 28 | 1 | 3 | 22 | 2 | 33 |
| H | −0.4574 | −2.89943 | 2.95812 | −1103 | 292 | −215 | 632 | −1691 | 308 | 35 | −1 | 0 | 22 | 9 | 31 |
| H | 0.38221 | −1.34891 | 2.85878 | −2658 | −530 | 918 | −732 | −3521 | 3574 | 33 | −1 | −1 | 46 | 20 | 23 |
| H | 1.1086 | −2.69966 | 3.72165 | −561 | −352 | 469 | 131 | −1088 | 663 | 30 | 1 | 1 | 29 | 5 | 36 |
| H | 2.60366 | −1.17663 | 1.51112 | 2568 | −2265 | 2376 | −1607 | −905 | −1332 | 25 | 13 | −3 | 48 | 4 | 30 |
| H | 3.28573 | −2.62549 | 0.77826 | 788 | −1399 | 358 | 127 | −283 | −787 | 33 | 8 | −3 | 26 | 2 | 33 |
| H | 3.15175 | −2.51671 | 2.52481 | 91 | −838 | 726 | −270 | −601 | −346 | 34 | 4 | 3 | 30 | 2 | 33 |
| H | 0.43171 | −4.94021 | 1.67127 | −486 | −152 | 25 | 932 | −414 | −318 | 31 | 3 | 1 | 25 | 1 | 29 |
| H | 1.94005 | −4.70724 | 2.54617 | −577 | −363 | 156 | 147 | −436 | −514 | 30 | −1 | 2 | 28 | −1 | 32 |
| H | 1.96169 | −4.83461 | 0.79132 | −270 | −487 | 84 | 804 | −211 | −439 | 27 | −1 | 0 | 22 | 3 | 34 |
| H | −0.42162 | −1.64235 | −2.70311 | −2463 | 616 | 863 | −71 | 3665 | 2611 | 39 | −4 | −2 | 37 | −19 | 24 |
| H | −1.24576 | −3.16841 | −2.38185 | −758 | 764 | 444 | 958 | 1424 | −128 | 42 | −3 | −4 | 18 | −5 | 29 |
| H | 0.04322 | −3.09931 | −3.58082 | −683 | −21 | −54 | 370 | 1161 | 540 | 32 | 0 | 0 | 27 | −4 | 36 |
| H | 2.07293 | −1.36254 | −2.04384 | 836 | −2367 | −2999 | −1019 | 1918 | 2 | 23 | 15 | 5 | 45 | −12 | 23 |
| H | 2.33409 | −2.80235 | −3.0336 | −233 | −708 | −676 | 39 | 847 | 79 | 32 | 4 | −3 | 28 | −4 | 33 |
| H | 2.95864 | −2.742 | −1.39344 | 421 | −1370 | −592 | 207 | 565 | −691 | 34 | 8 | 2 | 25 | −4 | 31 |
| H | 1.70628 | −4.92303 | −0.79188 | −331 | −422 | −85 | 849 | 211 | −442 | 28 | −1 | 3 | 22 | −2 | 33 |
| H | 1.20475 | −4.98264 | −2.4785 | −880 | −235 | −92 | 6 | 449 | −781 | 29 | 0 | −2 | 28 | 1 | 32 |
| H | −0.00816 | −5.0863 | −1.20662 | −501 | −46 | 26 | 970 | 313 | −408 | 32 | 2 | −1 | 24 | −1 | 28 |

**Table S8.** Fitting parameters of pNMR signals obtained with different computational methods.

| | | $\chi_{iso}$, Å³ | $\Delta\chi_{xx}$, Å³ | $\Delta\chi_{yy}$, Å³ | $\chi_{xz}$, Å³ | RMSE | Error degree of freedom |
|---|---|---|---|---|---|---|---|
| **B3LYP/def2-TZVP** | all signals | 0.069(1) | 0.040(3) | -0.03(1) | -0.01±0.03 | 36 | 14 |
| | selected | 0.069(1) | 0.040(3) | -0.03(1) | -0.02(1) | 6.38 | 6 |
| | selected | 0.068(1) | 0.036(4) | -0.04(1) | fixed at 0 | 10.5 | 7 |
| **TPSSH/def2-TZVP** | selected | 0.063(1) | 0.046(3) | -0.04(1) | 0.0003±0.006 | 6.35 | 6 |
| | selected | **0.063(1)** | **0.046(2)** | **-0.04(1)** | **fixed at 0** | **6.07** | **7** |
| **B3LYP/EPR-II** | selected | 0.069(1) | 0.040(3) | -0.03(1) | -0.007±0.007 | 6.37 | 6 |
| | selected | 0.069(1) | 0.037(2) | -0.03(1) | fixed at 0 | 6.15 | 7 |
| **BP86/def2-TZVP** | selected | 0.069(2) | 0.08(1) | -0.02±0.02 | -0.006±0.02 | 17.8 | 6 |
| | selected | 0.068(1) | 0.08(1) | -0.03(1) | fixed at 0 | 16.7 | 7 |
| **HF/def2-TZVP** | selected | could not reach a reasonable agreement with experiment | | | | 186 | 6 |

**Table S9.** Ligand field parameters calculated with CASSCF(6,5)/NEVPT2/def2-TZVP for 5 quintet, 45 triplet and 50 singlet states for X-Ray structure of the complex.

```
----------------------------
AILFT MATRIX ELEMENTS (NEVPT2)
----------------------------


E0                =  0.018882711 a.u. =   0.514 eV =   4144.3 cm**-1
H(dxy   ,dxy   )=  0.022269585 a.u. =   0.606 eV =   4887.6 cm**-1
H(dyz   ,dxy   )= -0.008951501 a.u. =  -0.244 eV =  -1964.6 cm**-1
H(dyz   ,dyz   )= -0.009372948 a.u. =  -0.255 eV =  -2057.1 cm**-1
H(dz2   ,dxy   )=  0.010316368 a.u. =   0.281 eV =   2264.2 cm**-1
H(dz2   ,dyz   )= -0.002174074 a.u. =  -0.059 eV =   -477.2 cm**-1
H(dz2   ,dz2   )=  0.005891424 a.u. =   0.160 eV =   1293.0 cm**-1
H(dxz   ,dxy   )= -0.026264992 a.u. =  -0.715 eV =  -5764.5 cm**-1
H(dxz   ,dyz   )=  0.008126089 a.u. =   0.221 eV =   1783.5 cm**-1
H(dxz   ,dz2   )= -0.016922601 a.u. =  -0.460 eV =  -3714.1 cm**-1
H(dxz   ,dxz   )=  0.029199490 a.u. =   0.795 eV =   6408.5 cm**-1
H(dx2-y2,dxy   )=  0.043447367 a.u. =   1.182 eV =   9535.6 cm**-1
H(dx2-y2,dyz   )= -0.004922911 a.u. =  -0.134 eV =  -1080.5 cm**-1
H(dx2-y2,dz2   )=  0.018012799 a.u. =   0.490 eV =   3953.4 cm**-1
H(dx2-y2,dxz   )= -0.047085588 a.u. =  -1.281 eV = -10334.1 cm**-1
H(dx2-y2,dx2-y2)=  0.065308713 a.u. =   1.777 eV =  14333.6 cm**-1
B                =  0.004634455 a.u. =   0.126 eV =   1017.1 cm**-1
C                =  0.014493589 a.u. =   0.394 eV =   3181.0 cm**-1 (C/B= 3.13)

The ligand field one electron eigenfunctions:
Orbital   Energy (eV)  Energy(cm-1)    dxy       dyz       dz2       dxz      dx2-y2
   1        0.000         0.0        0.385827  0.817483 -0.068328 -0.284001 -0.312304
   2        0.271      2187.2        0.235910  0.235612  0.642989  0.671387  0.156967
   3        0.341      2753.1        0.667697 -0.517675  0.107807 -0.033941 -0.522894
   4        0.499      4028.0       -0.398108 -0.030229  0.725561 -0.474701 -0.298022
   5        3.925     31653.9        0.437234 -0.085480  0.209371 -0.492027  0.718048
```

## S6 RELAXATION THEORY

This work deals with the rare case of NMR spectroscopy of a nucleus so close to the unpaired electron that (a) the point dipole approximation breaks down; (b) the contact part of the hyperfine coupling cannot be ignored. The system is also far outside the Zeeman limit in which most spin relaxation theories are formulated. Before we deal with the matter numerically, it is useful to review pre-existing – and now inapplicable – analytical results.

Solomon-Bloembergen-Morgan (SBM),[11–13] and Gueron ("Curie")[14] mechanisms assume an effective electron magnetic moment $\mu_{\text{eff}}$ (from the isotropic part of the susceptibility tensor) and use point-dipole approximation for the hyperfine coupling:[15]

$$R_1^{\text{dip}} = \frac{2}{15}\left(\frac{\mu_0}{4\pi}\right)^2 \frac{\gamma_N^2 \mu_{\text{eff}}^2}{r^6}\left[3j\left(\omega_N,\tau_{R,T_{1E}}\right) + 6j\left(\omega_E + \omega_N,\tau_{R,T_{2E}}\right) + j\left(\omega_E - \omega_N,\tau_{R,T_{2E}}\right)\right]$$

$$R_2^{\text{dip}} = \frac{1}{15}\left(\frac{\mu_0}{4\pi}\right)^2 \frac{\gamma_N^2 \mu_{\text{eff}}^2}{r^6}\begin{bmatrix}4j\left(0,\tau_{R,T_{1E}}\right) + 3j\left(\omega_N,\tau_{R,T_{1E}}\right) + 6j\left(\omega_E,\tau_{R,T_{2E}}\right) \\ +6j\left(\omega_E + \omega_N,\tau_{R,T_{2E}}\right) + j\left(\omega_E - \omega_N,\tau_{R,T_{2E}}\right)\end{bmatrix}$$

$$R_1^{\text{Curie}} = \frac{6}{5}\left(\frac{\mu_0}{4\pi}\right)^2 \frac{\omega_N^2 \mu_{\text{eff}}^4}{\left(3kT\right)^2 r^6} j\left(\omega_N,\tau_R\right) \tag{S1}$$

$$R_2^{\text{Curie}} = \frac{1}{5}\left(\frac{\mu_0}{4\pi}\right)^2 \frac{\omega_N^2 \mu_{\text{eff}}^4}{\left(3kT\right)^2 r^6}\left[4j\left(0,\tau_R\right) + 3j\left(\omega_N,\tau_R\right)\right]$$

where the spectral power density and the characteristic times are:

$$j\left(\omega,\tau\right) = \frac{\tau}{1+\omega^2\tau^2}, \qquad \tau_{R,T_{1E}} = \left(\frac{1}{\tau_R}+\frac{1}{T_{1E}}\right)^{-1}, \qquad \tau_{R,T_{2E}} = \left(\frac{1}{\tau_R}+\frac{1}{T_{2E}}\right)^{-1} \tag{S2}$$

Here, $\mu_0$ is vacuum permeability, $\gamma_N$ is the magnetogyric ratio of the nucleus, $\omega_N$ is the nuclear Zeeman frequency, $\omega_E$ is the electron Zeeman frequency, $\mu_{\text{eff}}$ is the effective magnetic moment of the electron, $r$ is the electron-nuclear distance, $\tau_R$ is the second rank rotational correlation time of what is often assumed to be isotropic rotational diffusion, $T_{1E}$ is the longitudinal electron relaxation time, and $T_{2E}$ is the transverse electron relaxation time.

When the unpaired electrons are delocalised and the nucleus is nearby, a point electron dipole is not a good approximation – the proper hyperfine tensor must be used instead:

$$R_1^{HF} = \frac{\Delta_A^2 S(S+1)}{90} \left[ 3j\left(\omega_N, \tau_{R,T_{1E}}\right) + 6j\left(\omega_E + \omega_N, \tau_{R,T_{2E}}\right) + j\left(\omega_E - \omega_N, \tau_{R,T_{2E}}\right) \right]$$

$$R_2^{HF} = \frac{\Delta_A^2 S(S+1)}{180} \left[ \begin{array}{l} 4j\left(0, \tau_{R,T_{1E}}\right) + 3j\left(\omega_N, \tau_{R,T_{1E}}\right) + 6j\left(\omega_E, \tau_{R,T_{2E}}\right) \\ + 6j\left(\omega_E + \omega_N, \tau_{R,T_{2E}}\right) + j\left(\omega_E - \omega_N, \tau_{R,T_{2E}}\right) \end{array} \right]$$

(S3)

where $\Delta_A^2$ is the second rank invariant of the hyperfine tensor:

$$\Delta_A^2 = a_{XX}^2 + a_{YY}^2 + a_{ZZ}^2 - a_{XX}a_{YY} - a_{XX}a_{ZZ} - a_{YY}a_{ZZ}$$
$$+ \frac{3}{4}\left[ \left(a_{XY} + a_{YX}\right)^2 + \left(a_{XZ} + a_{ZX}\right)^2 + \left(a_{YZ} + a_{ZY}\right)^2 \right]$$

(S4)

Eq (S1) is adequate at distances greater than 10 Å from the metal, and Eq (S3) is applicable at any distance in the Zeeman limit.

When the contact component of the hyperfine coupling is significant, an additional relaxation mechanism turns up: rapid electron relaxation creates stochastic noise in the isotropic hyperfine coupling operator, the resulting nuclear relaxation mechanism is called scalar relaxation of the second kind. It depends on the isotropic hyperfine coupling constant $A_{iso}$:[16]

$$R_1^{SRSK} = \frac{2A_{iso}^2 S(S+1)}{3} j\left(\omega_E - \omega_N, T_{2e}\right)$$

$$R_2^{SRSK} = \frac{A_{iso}^2 S(S+1)}{3} \left[ j\left(0, T_{1e}\right) + j\left(\omega_E - \omega_N, T_{2e}\right) \right]$$

(S5)

in this case, the role of correlation times is played by electron relaxation times.

More subtle effects appear in systems with significant susceptibility anisotropy.[17,18] For example, Curie mechanism pops an extra term due to the antisymmetry in the paramagnetic shielding tensor which arises from the combination of susceptibility anisotropy and hyperfine coupling anisotropy:[19,20]

$$R_1^{\text{Curie+CSA}} = \frac{1}{2}\Lambda_\sigma^2 \omega_N^2 \frac{\tau_R}{1+9\omega_N^2\tau_R^2} + \frac{2}{15}\Delta_\sigma^2 \omega_N^2 \frac{\tau_R}{1+\omega_N^2\tau_R^2}$$

$$R_2^{\text{Curie+CSA}} = \frac{1}{4}\Lambda_\sigma^2 \omega_N^2 \frac{\tau_R}{1+9\omega_N^2\tau_R^2} + \frac{1}{45}\Delta_\sigma^2 \omega_N^2 \left(4\tau_R + \frac{3\tau_R}{1+\omega_N^2\tau_R^2}\right)$$

(S6)

where $\Lambda_\sigma^2$ is the first rank invariant of the total chemical shielding tensor:

$$\Lambda_\sigma^2 = \left(\sigma_{XY} - \sigma_{YX}\right)^2 + \left(\sigma_{XZ} - \sigma_{ZX}\right)^2 + \left(\sigma_{YZ} - \sigma_{ZY}\right)^2 \tag{S7}$$

and the total shielding tensor is the sum of the diamagnetic and paramagnetic contributions:

$$\boldsymbol{\sigma} = \boldsymbol{\sigma}_0 - \chi\mathbf{A} \tag{S8}$$

A notable case was recently described where the negative sign in this equation resulted in a reduction of shielding anisotropy, and thus a slowdown in the nuclear relaxation.[21]
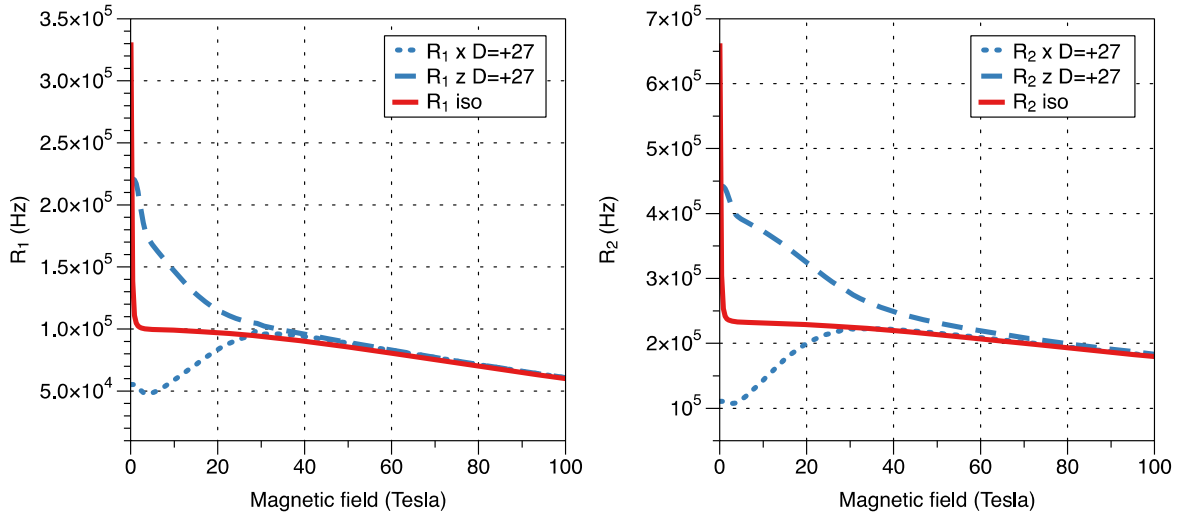


**Figure S8.** Simulated contact/dipolar relaxation rates (longitudinal – $R_1$, and transverse – $R_2$) as a function of magnetic field. The model represents a point paramagnetic centre with S = 1 and $^1$H located 1.57 Å away along either along x-axis (dotted lines) or z-axis (dashed lines) and an axial ZFS with $D$ = +27 cm$^{-1}$. The g-tensor is assumed to be isotropic with $g$ = 2, and electron relaxation rate is $3.3 \times 10^{10}$ s$^{-1}$.

# S7 LITERATURE

[1] J. C. Ott, H. Wadepohl, M. Enders, L. H. Gade, *J. Am. Chem. Soc.* **2018**, *140*, 17413–17417.

[2] M. J. Frisch, G. W. Trucks, H. B. Schlegel, G. E. Scuseria, M. A. Robb, J. R. Cheeseman, G. Scalmani, V. Barone, G. A. Petersson, H. Nakatsuji, et al., **2016**.

[3] Y. Zhao, D. G. Truhlar, *J. Phys. Chem. A* **2008**, *112*, 6794–6799.

[4] a) F. Neese, *WIREs Comput. Mol. Sci.* **2012**, *2*, 73–78. b) F. Neese, *WIREs Comput. Mol. Sci.* **2018**, *8*, 4–9.

[5] A. G. Webb, in *Annu. Rep. NMR Spectrosc.*, Academic Press, **2002**, pp. 1-67.

[6] K. Holldack, A. Schnegg, *J. large-scale Res. Facil. JLSRF* **2016**, *2*, A51.

[7] A. Schnegg, J. Behrends, K. Lips, R. Bittl, K. Holldack, *Phys. Chem. Chem. Phys.* **2009**, *11*, 6820.

[8] J. Nehrkorn, K. Holldack, R. Bittl, A. Schnegg, *J. Magn. Reson.* **2017**, *280*, 10–19.

[9] S. Stoll, A. Schweiger, *J. Magn. Reson.* **2006**, *178*, 42–55.

[10] J. Nehrkorn, J. Telser, K. Holldack, S. Stoll, A. Schnegg, *J. Phys. Chem. B* **2015**, *119*, 13816–13824.

[11] I. Solomon, *Phys. Rev.* **1955**, *99*, 559–565.

[12] N. Bloembergen, *J. Chem. Phys.* **1957**, *27*, 572–573.

[13] N. Bloembergen, L. O. Morgan, *J. Chem. Phys.* **1961**, *34*, 842–850.

[14] M. Gueron, *J. Magn. Reson.* **1975**, *19*, 58–66.

[15] I. Bertini, C. Luchinat, G. Parigi, Eds. , *Solution NMR of Paramagnetic Molecules: Applications to Metallobiomolecules and Models*, Elsevier, New York, **2016**.

[16] A. Abragam, *The Principles of Nuclear Magnetism*, Oxford University Press, London, **1961**.

[17] E. A. Suturina, I. Kuprov, *Phys. Chem. Chem. Phys.* **2016**, *18*, 26412–26422.

[18] L. Lang, E. Ravera, G. Parigi, C. Luchinat, F. Neese, *J. Phys. Chem. Lett.* **2020**, *11*, 8735–8744.

[19] E. A. Suturina, K. Mason, C. F. G. C. Geraldes, N. F. Chilton, D. Parker, I. Kuprov, *Phys. Chem. Chem. Phys.* **2018**, *20*, 17676–17686.

[20] A. J. Vega, D. Fiat, *Mol. Phys.* **1976**, *31*, 347–355.

[21] H. W. Orton, I. Kuprov, C.-T. Loh, G. Otting, *J. Phys. Chem. Lett.* **2016**, *7*, 4815–4818.